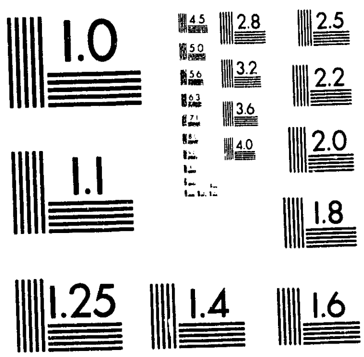
1.0
1.1
1.25
1.4
1.6
1.8
2.0
2.2
2.5
2.8
3.2
3.6
4.0

1 of 1

ANL/FC/CP--78624
CONF-930830--25

1993 National Heat Transfer Conference
Atlanta, Georgia, August 8-11

A Parametric Study of Heat Transfer Within a Planar Thermosyphon

Randy Clarksean
and
Greg Phillips
Fuel Cycle Division
Argonne National Laboratory
P.O. Box 2528
Idaho Falls, Idaho 83403

Abstract

The results of a parametric study for a planar thermosyphon are presented. The thermosyphon consists of a "U-shaped" geometry, with the center portion of the "U" being a solid. The outer legs of the "U" are the flow channels. One of the outer surfaces of a channel was held at a constant temperature. The remaining outer surfaces were considered adiabatic. The configuration described is characteristic of passive systems for radioactive waste storage and reactor safety systems. Parameters which were varied included the channel geometry, the thermal conductivity of the solid, and the Ra number. The average Nu number for the constant temperature surface decreased as the inlet channel width decreased, and as the thermal conductivity of the solid increased. A modified Ra number, defined as the Ra number divided by the length to gap ratio for the outer channel, is used in the paper. At low values of the modified Ra number, there is over an order of magnitude decrease in the average Nu number for a change in the inlet channel width from 1.0 to 0.25. But as the value of the modified Ra number increases for any inlet channel width, the average Nu number results approached those of vertical parallel plates, independent of the inlet channel width and the thermal conductivity of the solid. The vertical parallel plate data is approached because the boundary layer flow near the heated plate is unaffected by the surface of the intervening solid.

Nomenclature

b = *nondimensional outlet channel width*, 1.
B = *outlet channel width.*
C_p = *specific heat.*
$\vec{g}$ = *gravity vector.*
g = *gravity force.*
k = *thermal conductivity of fluid.*
K = *ratio of solid to fluid thermal conductivities.*
l = *system height.*
L = *nondimensional system height*, $\frac{l}{B}$.
Nu = *Nusselt number*, $\frac{q''B}{(T_w - T_o)k}$.
p_m = *motion pressure field.*
Pr = *Prandtl number.*
q'' = *heat flux along the heated wall.*
Ra = *Rayleigh number, see Equation* 13.
T = *temperature.*
T_o = *inlet fluid temperature.*
T_w = *heated wall temperature.*
$\vec{u}$ = *velocity vector.*
$\vec{u}^*$ = *nondimensional velocity, see Equation* 9.
W = *inlet channel width.*
w = *nondimensional inlet channel width*, $\frac{W}{B}$.
x = *horizontal location.*
x^* = *nondimensional horizontal location*, $\frac{x}{B}$.
y = *vertical location.*

y^* = *nondimensional vertical location*, $\frac{y}{B}$.

α = *thermal diffusivity.*

β = *coefficient of volume expansion.*

ρ = *density.*

ρ_o = *density at reference temperature.*

μ = *absolute viscosity.*

ν = *kinematic viscosity.*

θ = *nondimensional temperature, see Equation* 10.

1 Introduction

Thermosyphons are used in a variety of applications. The applications include the cooling of electronic components (Reference [1] for an example), heat removal systems for nuclear reactors (References [2] and [3]), solar energy systems (Reference [4]), and other industrial applications. The use of thermosyphons, which are sometimes referred to as passive systems, has increased because they are less expensive than forced cooling systems. Passive systems are less expensive because they do not require blowers or pumps for fluid circulation. In addition, passive systems are more dependable because they operate without any external control signals or power, which insures they will continue to function under all operating conditions. Thermosyphons only rely on the heat generated within the system to move fluid through the system.

Recent reviews of several types of thermosyphons can be found in References [5] and [6]. The general system under consideration here is an open loop thermosyphon with a constant temperature reservoir. The system is "U-shaped," with the outer surface of one leg of the "U" held at an elevated constant temperature. Buoyancy forces are generated along the heated surface. The buoyant forces cause flow to enter one leg of the system, and to exit from the heated leg of the system. In general, depending on the location of the heat source within the system, the flow may be oscillatory or steady. Recent examples of analyses for open loop thermosyphons can be found in References [7] and [8]. Each of the systems analyzed in these references contained cylindrical ducts for the flow passages.

The recent experimental work in Reference [9] discussed an open loop thermosyphon with cylindrical annuli as flow passages. The results of that work indicated that the local heat transfer coefficients for heated surfaces could be related to heat transfer relationships for a single vertical plate (or vertical cylinders). The results

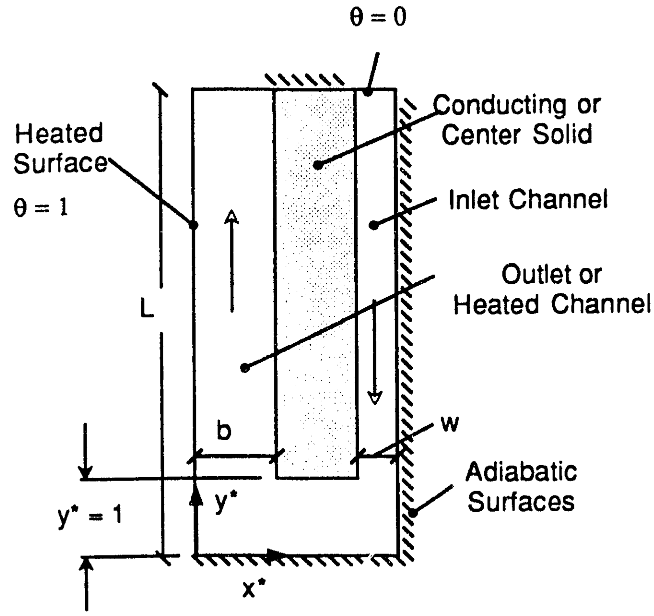

Figure 1: Schematic of planar thermosyphon and the assigned boundary conditions.

of Reference [9] generated the interest in the present work.

For the system analyzed here (see Figure 1), there are two sets of vertical parallel plates connected by an intervening solid. The vertical channels are connected by a flow channel between the bottoms of the two sets of plates. One of the sets of parallel plates has a heated surface. The heat transfer off of the heated surface in the thermosyphon should be similar in nature to that of heated vertical parallel plates. A variety of work has been conducted on heated vertical parallel plates. Examples of natural convection between vertical parallel plates can be found in References [10] - [13].

The intent of the present work is to determine what impact channel geometry, thermal conductivity of the solid between the flow channels, and the Ra number have on the overall heat transfer from the system.

2 Problem Definition

The geometry to be analyzed is shown in Figure 1. The nondimensional lengths are w for the inlet channel width, and b for the outlet or heated channel width. The total nondimensional height of the system is L. The thermal conductivity of the solid between the inlet and outlet channels is varied.

The flow within this system relies only on the buoyancy forces generated by the heated surface within the system. As the fluid becomes buoyant along the heated surface, fluid is drawn into the inlet channel. The system relies only on natural convection for heat removal. The solid between the inlet and outlet, or heated, channels has a thermal conductivity.

Figure 1 shows the problem geometry and the appropriate boundary conditions. All of the walls are considered no-slip (velocities set equal to zero). The specification of the boundary conditions for the inlet and outlet are more involved. The normal component of the stress tensor at the inlet and outlet boundaries is defined as

$$\sigma_n = -P + \mu(u_{i,j} + u_{j,i})n_i n_j \tag{1}$$

The natural boundary condition for the finite element method forces σ_n to be equal to zero. Normally this forces the pressure P to be close to zero. For the inflow boundary condition this appropriate, at the outflow, this boundary condition can cause problems. *FIDAP* alleviates this problem by including the integral of pressure over the outflow boundary on the global system of equations to be solved. At each iteration of the solution procedure the integral is updated until convergence is obtained (see Reference [15]).

For the current problem, the nondimensional temperature of the fluid entering the inlet channel is assumed to be constant, $\theta = 0$. The heated surface is assigned a temperature of $\theta = 1$. All of the surfaces marked with cross-hatching are considered adiabatic. The interaction of the fluid and solid results in a conjugate heat transfer problem. The conduction of energy within the solid and the flow past the surfaces are coupled. To simplify the problem, radiative heat transfer between the surfaces was assumed to be negligible.

3 Governing Equations and Numerical Techniques

The governing equations for the natural convection of an incompressible fluid are the continuity, momentum, and energy equations. The governing equations are shown below.

$$\nabla \cdot \vec{u} = 0 \tag{2}$$

$$\rho(\vec{u} \cdot \nabla)\vec{u} = -\nabla p + \mu \nabla^2 \vec{u} + \rho \vec{g} \tag{3}$$

$$\rho C_p \vec{u} \cdot \nabla T = k \nabla^2 T \tag{4}$$

Using the Boussinesq approximation, the momentum equation becomes

$$\rho(\vec{u} \cdot \nabla)\vec{u} = -\nabla p_m + \mu \nabla^2 \vec{u} + \rho g \hat{j} \beta (T - T_o) \tag{5}$$

The following definitions were used to nondimensionalize the governing equations:

$$x^* = \frac{x}{B} \tag{6}$$

$$y^* = \frac{y}{B} \tag{7}$$

$$U_{ref} = \frac{\alpha}{B}\sqrt{Ra\ Pr} \tag{8}$$

$$\vec{u}^* = \frac{\vec{u}}{U_{ref}} \tag{9}$$

$$\theta = \frac{(T - T_o)}{(T_w - T_o)} \tag{10}$$

$$p^* = \frac{p_m\ B}{\mu\ U_{ref}} \tag{11}$$

$$Pr = \frac{\nu}{\alpha} \tag{12}$$

$$Ra = \frac{g\beta(T_w - T_o)B^3}{\alpha\nu} \tag{13}$$

The characteristic length of the problem was selected to be the gap width of the outlet or heated channel. The gap width of the heated channel was selected so the heat transfer off the heated wall could be compared to vertical parallel plate data. The characteristic reference velocity and pressure are the typical definitions used for vertical parallel plates or single vertical plates (see Reference [6]).

Using the above definitions, the nondimensional form of the governing equations can be shown to be

$$\nabla \cdot \vec{u}^* = 0 \tag{14}$$

$$\sqrt{\frac{Ra}{Pr}}(\vec{u}^* \cdot \nabla)\vec{u}^* = -\nabla p^* + \nabla^2 \vec{u}^* + \sqrt{\frac{Ra}{Pr}}\theta \tag{15}$$

$$\sqrt{\frac{Ra}{Pr}}\vec{u}^* \cdot \nabla\theta = \nabla^2\theta \tag{16}$$

All of the numerical results were generated by the use of the general purpose finite element code *FIDAP* (see Reference [15]). *FIDAP* uses a Galerkin formulation of the problem, and uses the penalty method approach to solve the incompressible flow problem. The resultant matrix formulation for the natural convection problem being analyzed here was then iteratively solved by a combination of the quasi-newton method (sometimes referred to as the matrix update method) and successive substitution method.

Reference [15] contains a variety of examples problems to demonstrate the ability of *FIDAP* to model different flow situations. One of the example problems analyzes natural convection between vertical parallel plates. Comparison of the results in the example with previously published work indicates there is less than a one percent error between *FIDAP* and the work of Reference [13]. The example problem used approximately 1100 nodes for a *Ra* number ranging from 100 to 3×10^5.

For the current problem, over twice as many nodes were used to discretize the two channel flowfield. A set of analyses were conducted to demonstrate that the results were independent of the grid selected. Less than a one percent change in the average *Nu* number occurred when the mesh was increased from 2383 to 4133 nodes for all of the channel lengths under consideration.

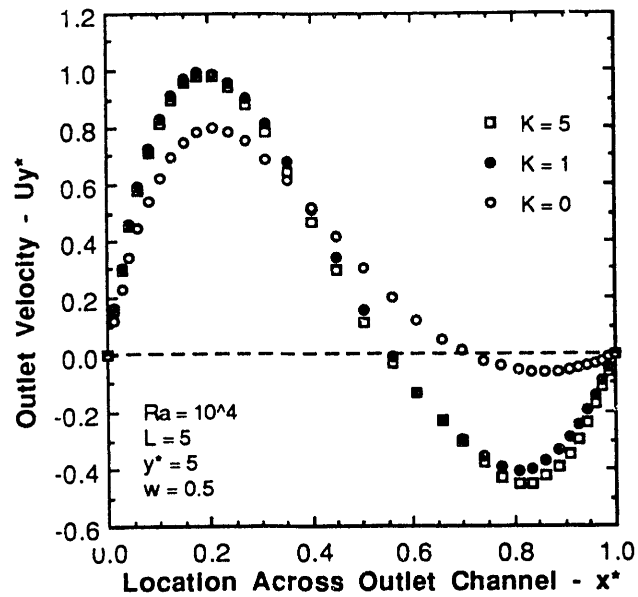

Figure 4: Effect of K on the outlet velocity profile for $Ra = 10^4$, $L = 5$, and $w = 0.5$.

4 Discussion of Results

The inlet width w, system length L, ratio of solid to fluid thermal conductivity K, and the *Ra* number were the parameters varied in this study. The *Pr* was set to a constant value of 0.71, to represent air as the working fluid. The inlet channel width w was varied from 0.25 to 1. The length of the system varied between 2 and 60. The ratio of solid to fluid thermal conductivity ranged from 0 to 10. The conductivity ratio was varied over this range because this is typical for the application discussed in Reference [9]. The *Ra* numbers ranged between 10^2 and 3×10^4, and were selected to show the wide variation in *Nu* when compared to vertical parallel plate data. Representative results are discussed below.

The effect of the solid thermal conductivity and *Ra* number on the streamlines and isotherms are shown in Figures 2 and 3. The length of the system was selected to be 5. In general, as the thermal conductivity of the solid increases for a constant *Ra* number, the amount of recirculating flow in the heated or outlet channel increases. An increase on the amount of fluid being recirculated is indicated by the number of streamlines that start and finish on the flow outlet.

As the thermal conductivity of the solid increases, the amount of energy which can be removed from the flow stream near the center solid increases. Removing more energy from the flow stream near the center solid decreases the temperature of the fluid near the center wall. As the temperature of the fluid decreases near the center solid, there is a bigger temperature differential across the fluid in the outer channel. The increase in temperature differential results in an increase in the "effective" *Ra* number across the outer channel, which would allow for more vigorous recirculation. The "effective" *Ra* number refers to the buoyancy force which is generated between the heated plate and the center solid in the outer channel. A larger temperature differential increases the amount of fluid entering the top of the outer channel.

The increase in flow recirculation is supported by an examination of the velocity profiles at the top of the outlet channel (see Figure 4). There is an increase in the amount of fluid being recirculated as K changes from 0 (insulated surface) to 1. There is a smaller increase in flow recirculation as K changes from 1 to 5. Future work will be conducted to insure that the outlet boundary condition is not impacting the amount of fluid recirculation. The inlet and outlet boundaries will be changed by adding a plenum region above each channel.

As the *Ra* number increases, for a fixed thermal conductivity ratio K, the amount of preheating of the inlet flow stream decreases. This effect is noted by the movement of the isotherms away from the inlet and movement closer to the heated surface as shown in Figure 3. Less energy is transported to the incoming flow because

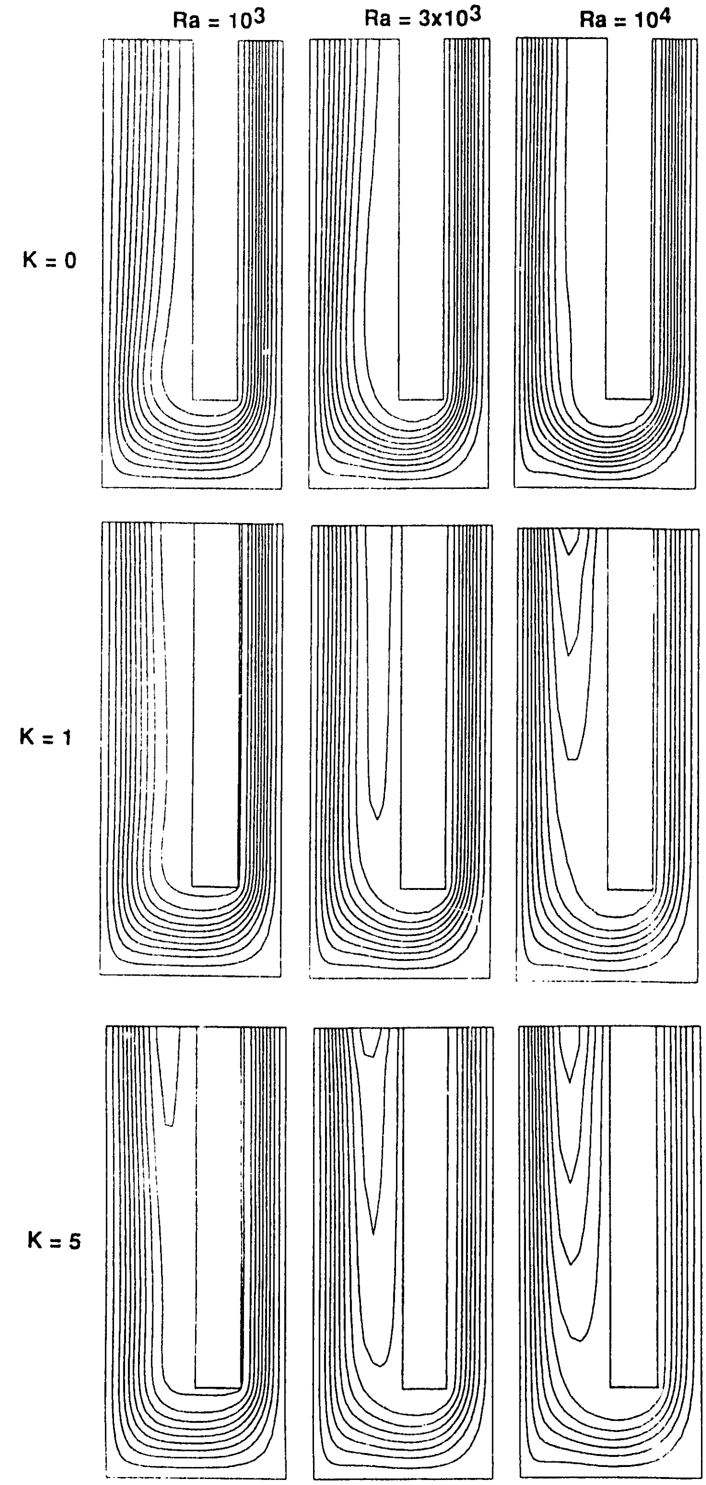

Figure 2: Effect of K and Ra number on streamlines for $L = 5$ and $w = 0.5$.

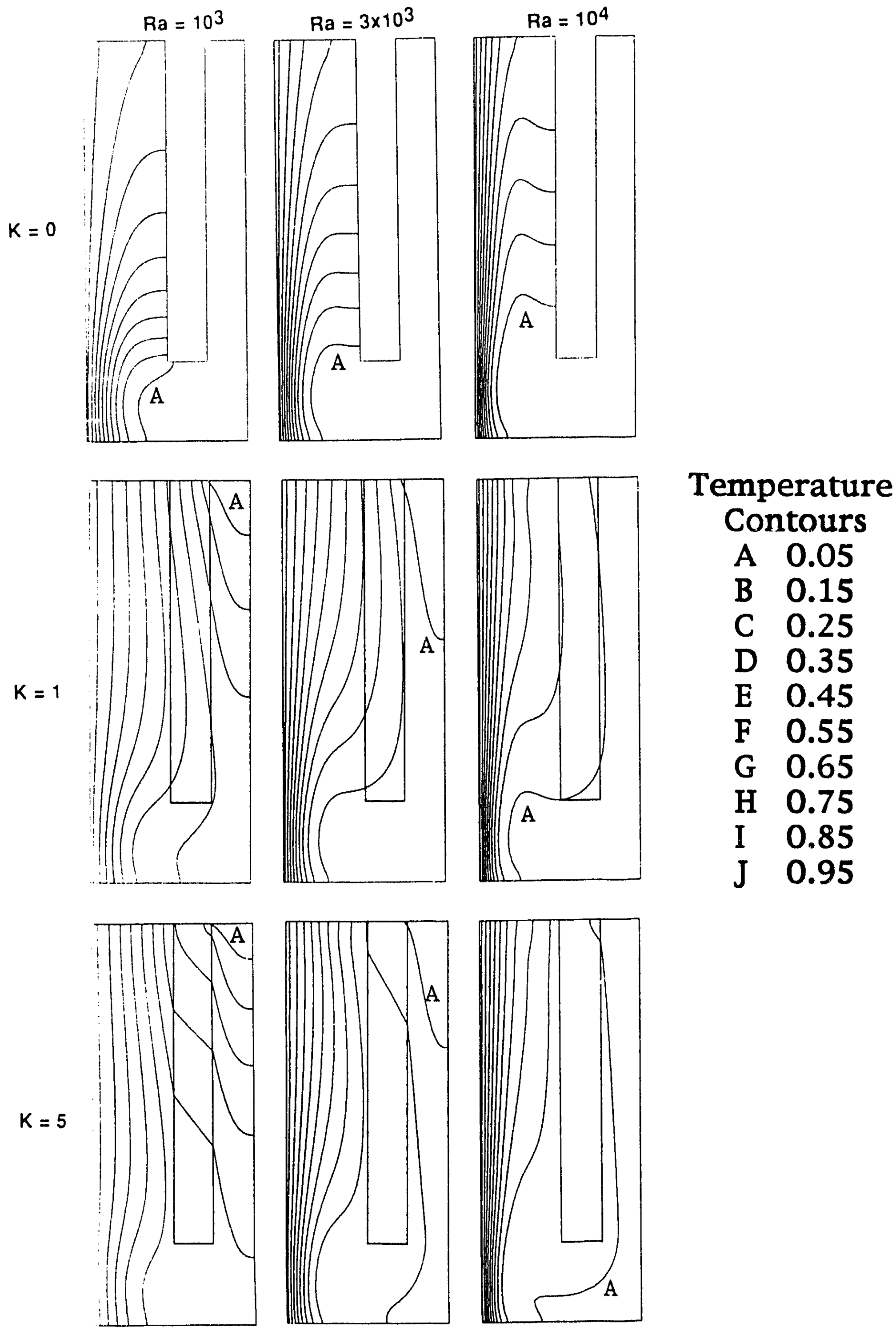

Figure 3: Effect of K and Ra number on isotherms for $L = 5$ and $w = 0.5$.

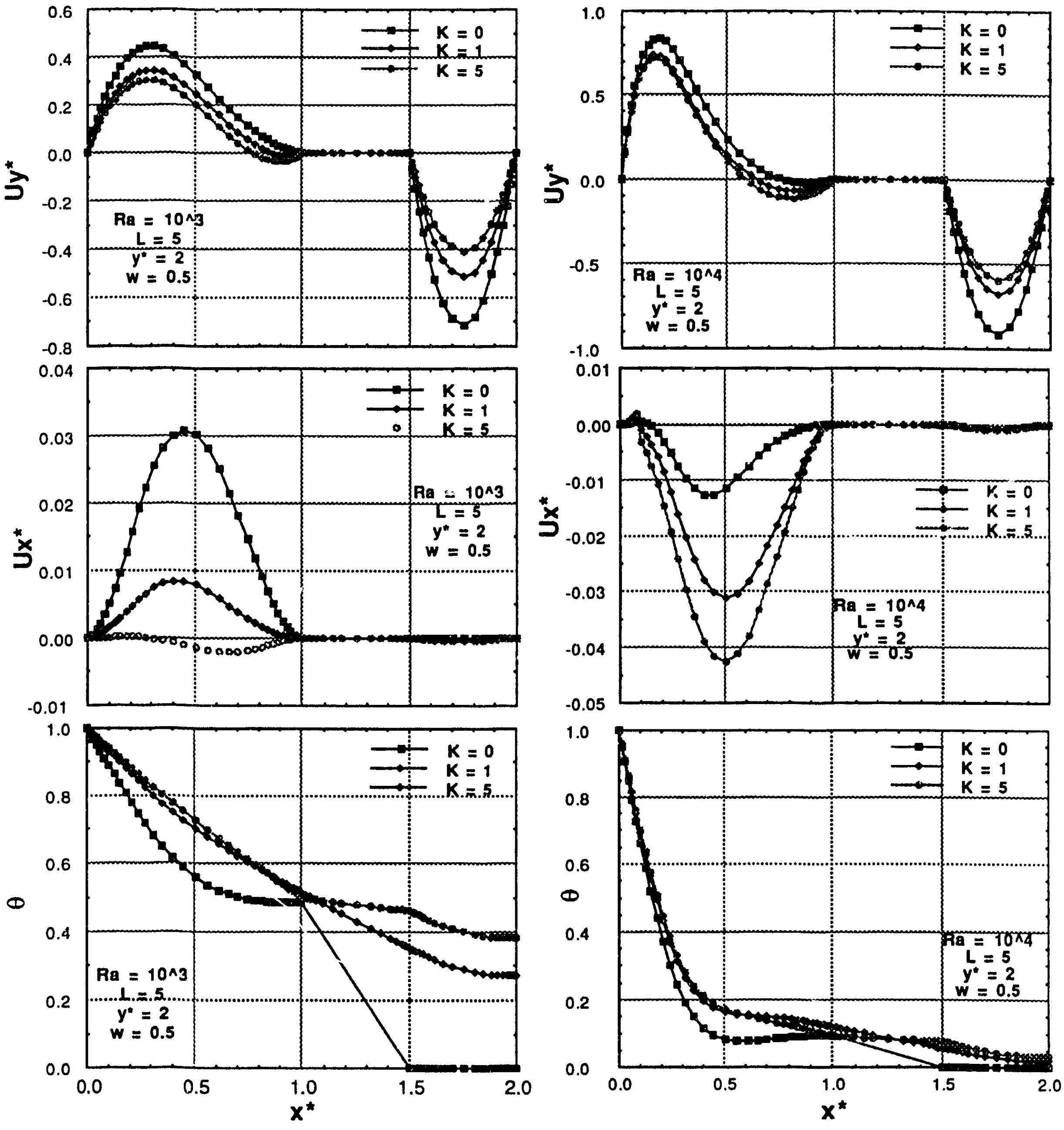

Figure 5: Velocity and temperature profiles for variations in K ($Ra = 10^3$ left side and $Ra = 10^4$ right side, $L = 5$, and $w = 0.5$ at $y^* = 2$).

a boundary layer type flow develops near the heated surface. As the Ra number increases, the majority of the flow stays near the heated surface, only allowing fluid with a lower temperature near the center solid (conducting solid).

Velocity and temperature profiles were also examined at $y^* = 2$ to see what effect the solid has on the flowfield. The x and y components of the velocity and the temperatures are shown for both flow channels in Figure 5. The Ra numbers are 10^3 and 10^4 respectively. For $K = 0$, the flow in the inlet channel is fully-developed ($u_x^* = 0$) for both sets of data. But for $K = 1$ or $K = 5$ the amount of energy transported across the solid is non zero. The addition of energy to the inlet channel only results in a small change in the u_x^* velocity component. The flow can still be considered fully-developed, but as the length of the channel increases, it is anticipated the flow will become thermally developing as more energy is transported to the inlet flow.

For both Ra numbers, the amount of flow through the system decreases as the thermal conductivity ratio of the solid increases. The total flow through the system is represented by the integral of the u_y^* profile. The decrease in total flow is indicated by the decrease in the magnitude of u_y^* (for similar profiles) as K increases. This decrease in u_y^* is the result of two effects, the increase in heat transfer across the solid, and the increased amount of recirculation in the outer channel.

The increase in heat transfer across the solid results in a small increase in negative buoyancy effects on the inlet flow channel. The heat transfer across the solid also preheats the fluid entering the outlet channel. The increase in negative buoyancy effects results in an increased flow resistance. Preheating the fluid before it enters the outer channel results in a decreased temperature difference between the fluid approaching the heated wall and the heated wall. Decreasing this temperature decreases the "effective" Ra number, which results in a decrease in the buoyancy force which drives the flow through the system. The "effective" Ra number in this instance refers to the buoyancy force generated between the heated fluid at the entrance to the heated channel and the heated wall itself.

The variation in the local Nu number for the heated surface as a function of the thermal conductivity ratio can be found in Figure 6. Representative results for Ra numbers of 10^3 and 10^4 are shown. In general, the local Nu decreases as the thermal conductivity of the solid increases. An exception to this conclusion occurs for the $Ra = 10^3$ data. As energy is removed from the flow stream in the heated channel along the conducting solid, a greater temperature difference exists across the fluid in the heated channel. A larger temperature gradient results in an increase in the local heat transfer.

The variation of the average Nu number as a function of the quantity $Ra\frac{b}{L}$ is shown in Figure 7. The effect of the width of the outlet channel and the overall length are not independent parameters, but are coupled in the ratio $\frac{b}{L}$. The usage of the quantity $Ra\frac{b}{L}$ is consistent with the results presented in References [10], [11], and [13]. All of the results shown in Figure 7 are for $K = 0$.

The Nu number relationships for the vertical parallel plates shown in Figure 7 were taken from Reference [10]. Reference [10] analyzed natural convection between heated vertical parallel plates. For the parallel plates, one of the surfaces was isothermally heated, and the other was adiabatic. The dashed lines represent the average Nu number limits for high and low Ra numbers for vertical parallel plates. At low Ra numbers, the steepest of the two dashed lines represents the fully-developed solution. The authors of Reference [10] concluded that for the flow between vertical parallel plates to approach a fully-developed condition, the value of $Ra\frac{b}{L}$ would be approximately 3 or 4. The limiting Nu number relationship for the parallel plates at the higher $Ra\frac{b}{L}$ ratios was only found to be approximately 10 percent higher than the single vertical plate relationship. In general, the small difference in average Nu numbers indicates that parallel plate data can be approximated by relationships for single vertical plates at high $Ra\frac{b}{L}$ values.

Three different inlet channel widths were evaluated in the present study. The inlet channel widths were $w = 1$, 0.5, and 0.25. There is a good correlation between the average Nu numbers for each of the different channel widths, independent of the channel length. The correlations only depend on the quantity $Ra\frac{b}{L}$. The results shown in Figure 7 are for system lengths ranging from 2 to 60.

The results shown in Figure 7 indicate that the average Nu number decreases as the inlet channel width decreases for low values of $Ra\frac{b}{L}$. The decrease in the average Nu number is the result of decreased flow into the system for the lower Ra numbers. The amount of flow entering the system decreases because there is an increase in flow restriction, and because the inlet flow stream is preheated. The "preheating" of the inlet flow results in negative buoyancy forces, which can further restrict the amount of flow entering the system.

At higher values of $Ra\frac{b}{L}$, the results indicate that the average Nu number is relatively independent of the inlet channel width. At higher Ra numbers, the buoy-

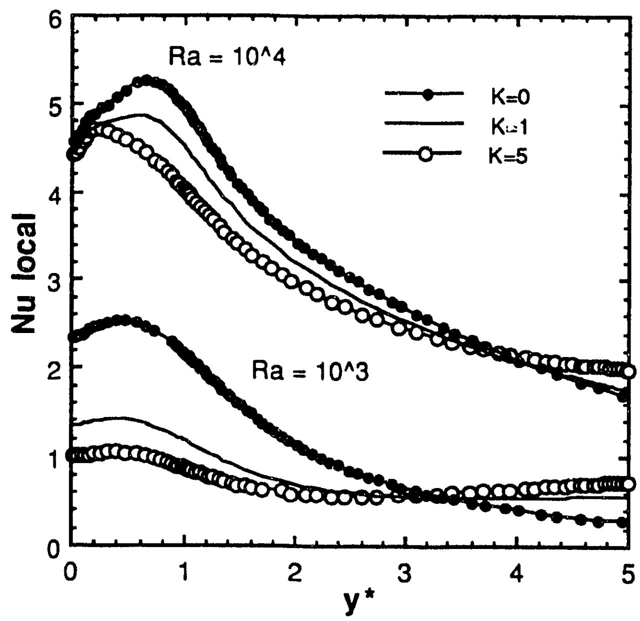

Figure 6: Changes in local Nu from variations in K for $L = 5$, and $w = 0.5$.

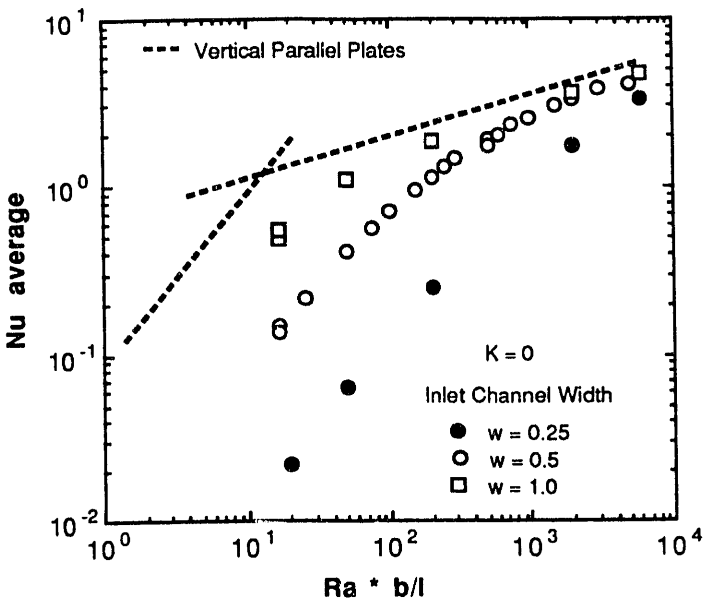

Figure 7: Variation in the average Nu number as a function of $Ra\frac{b}{L}$ for $K = 0$ - changes in channel geometry.

ancy forces generated within the system become much greater than the forces restricting the flow. In addition, the heat transfer off the heated surface approaches the average Nu number for the vertical parallel plates. At this point, the heat transfer off the heated surface is relatively independent of the adjacent surface. The heat transfer is independent of the other parallel surface because the boundary layer is not greatly affected.

The last item of interest is the effect of thermal conductivity on the average Nu number. Figure 8 shows that the average Nu number decreases by approximately 40 to 50 percent for the lower values of $Ra\frac{b}{L}$. But at higher $Ra\frac{b}{L}$ values, the average Nu number is only slightly modified. Once again these results indicate that at higher values of $Ra\frac{b}{L}$, the heat transfer off the heated surface approaches the vertical parallel plate data.

The average Nu number for the heated surface should approach the vertical flat plate data at large values of $Ra\frac{b}{L}$. The results indicate that if the value of $Ra\frac{b}{L}$ is on the order of 10^4 or greater, the amount of heat transfer off the heated surface will be approximately the same as it is for vertical parallel plates. The heat transfer off the heated surface, for a given inlet channel width, is considered to be "maximized" if it approaches the vertical parallel plate results. It is "maximized" in the sense that by increasing the inlet channel width will not significantly increase the amount of heat transfer from the system. From a thermosyphon design standpoint, this is an important conclusion, because a system can be optimized by insuring that $Ra\frac{b}{L}$ is sufficiently large. Caution should be taken in relying only on this relationship. For example, the inlet channel has to be large enough to allow flow to occur through the system. If the inlet channel is too small, the outer channel will act like a cavity with small recirculation cells being setup. Further analysis will be conducted to determine if a relationship can be developed to bracket this type of "flow" or "no-flow" situation.

5 Conclusions and Future Work

The heat transfer within a "U" shaped planar thermosyphon has been analyzed. Several parameters were varied. The parameters included the inlet channel width, the length of the channels, the thermal conductivity of the solid, and the Ra number.

The results have been compared with vertical parallel plate data. As the value of $Ra\frac{b}{L}$ approaches 10^4, the average Nu number data approaches the results for vertical parallel plates. The approach to the vertical plate data indicates that the effect of the inlet channel width and the thermal conductivity of the intervening

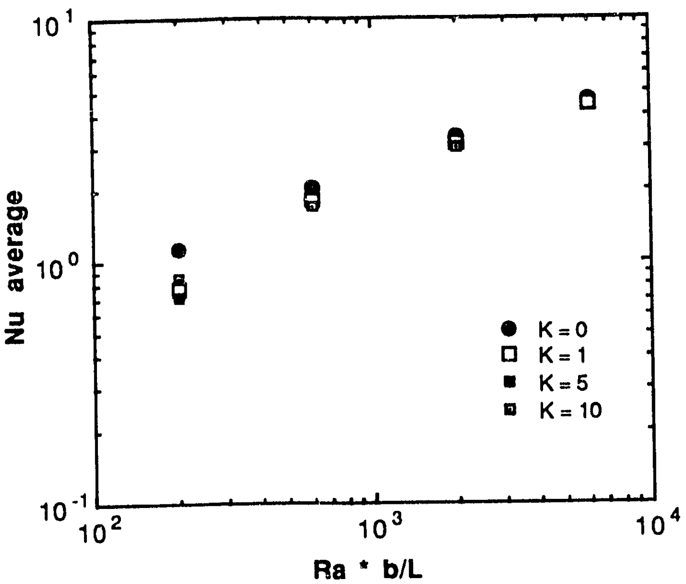

Figure 8: Variation in the average Nu number as a function of $Ra\frac{b}{L}$ for $K = 0,\ 1,\ 5,\ 10$ for $L = 5$, and $w = 0.5$.

solid have little impact on the overall heat transfer from the system at high $Ra\frac{b}{L}$ numbers. At low $Ra\frac{b}{L}$ values, there is over an order of magnitude decrease in the average Nu number for a change in the inlet channel width from 1.0 to 0.25. Increasing the thermal conductivity of the solid at low $Ra\frac{b}{L}$ values results in a 40 to 50 percent decrease in the average Nu number. The reduction of the average Nu number is a decrease when compared to the $K = 0$ data, not when compared to the vertical parallel plate data.

Future work will consider:

- The effects of radiative heat transfer between the surfaces in the system.
- The addition of a plenum region above the inlet and outlet channels to more realistically model the inlet and outlet flows.
- The evaluation of the local Nu numbers on the surfaces of the solid separating the two flow channels.
- The use of a constant heat flux boundary condition.

Acknowledgments

This work was supported by the U.S. Department of Energy, Nuclear Energy Programs, under contract no.

References

[1] Lin, T.-Y., and Hsieh, S.-S., "Natural Convection of Opposing/Assisting Flows in Vertical Channels with Asymmetrically Discrete Heated Ribs," *International Journal of Heat and Mass Transfer*, vol. 33, no. 10, pp. 2295-2309, 1990.

[2] Beine, B., Kaminski, V., and von Lensa, W., "Integrated Design of Prestressed Cast-Iron Pressure Vessel and Passive Heat Removal System for the Reactor Cell of a 200 MWth Modular Reactor," *Nuclear Engineering and Design*, vol. 136, pp. 135-141, 1992.

[3] Kwant, W., and Boardman, C.E., "PRISM-Liquid Metal Cooled Reactor Plant Design and Performance," *Nuclear Engineering and Design*, vol. 136, pp. 111-20, 1992.

[4] Mazria, E., The Passive Solar Energy Book, Rodale Press, Emmaus, PA, 1979.

[5] Mertol, A., and Greif, R., "A Review of Natural Circulation Loops," in *Natural Convection Fundamentals and Applications*, edited by Kakac, C., Aung, W., and Viskanta, R., Hemisphere Publishing Corporation, Washington, 1985.

[6] Gebhart, B., Jaluria, Y., Mahajan, R.L., and Sammakia, B., Buoyancy-Induced Flows and Transport, Hemisphere Publishing Corporation, Washington, D.C., 1988.

[7] Torrance, K.E., "Open-Loop Thermosyphons with Geological Applications," *ASME Journal of Heat Transfer*, vol. 101, pp. 677-683, 1979.

[8] Bau, H.H., and Torrance, K.E., "Transient and Steady Behavior of an Open, Symmetrically-Heated, Free Convection Loop," *International Journal of Heat and Mass Transfer*, vol. 24, no. 4, pp. 597-609, 1981.

[9] Clarksean, R.L., "Experimental Analysis of Natural Convection Within a Thermosyphon," Third World Conference on Experimental Heat Transfer, Fluid Mechanics and Thermodynamics, Honolulu, Hawaii, October 31 to November 5, 1993.

[10] Miyatake, O., and Fujii, T., "Free Convective Heat Transfer Between Vertical Parallel Plates-One Plate Isothermally Heated and the Other Thermally Insulated," *Heat Transfer-Japanese Research*, vol. 3, pp. 30-8, 1972.

[11] Miyatake, O., Fujii, T., Fujii, M., and Tanaka, H., "Natural Convective Heat Transfer Between Vertical Parallel Plates-One Plate With a Uniform Heat Flux and the Other Thermally Insulated," *Heat Transfer-Japanese Research*, vol. 4, pp.25-33, 1973.

[12] Naylor, D., Floryan, J.M., and Tarasuk, J.D., "A Numerical Study of Developing Free Convection Between Isothermal Vertical Plates," *Transactions of the ASME, Journal of Heat Transfer*, vol. 113, p. 620-6, August, 1991.

[13] Aung, W., Fletcher, L.S., and Sernas, V., "Developing Laminar Free Convection Between Vertical Flat Plates with Asymmetric Heating," *International Journal of Heat and Mass Transfer*, vol. 15, pp. 2293-308, 1972.

[14] Bejan, A., Convection Heat Transfer, John Wiley and Sons, New York, 1984.

[15] FIDAP Users Manual, Revision 6.0, Fluid Dynamics International, Evanston, Illinois, April 1991.

DATE

FILMED

10/25/93

END